International Journal of Biotech Trends and Technology
ISSN: 2249 – 0183 /doi:10.14445/22490183/IJBTT-V10I4P604

Volume 10 Issue 4, 30-37, Oct-Dec 2020

Contactless Cardio Monitor: a Contactless Cardiovascular Monitoring Software

Lucas Macedo da Silva [#1], Pedro Henrique de Brito Souza [*2], Adson Ferreira da Rocha [*3], Talles Marcelo G. de A. Barbosa [#4]

[#] *Pontifical Catholic University of Goiás, Goiânia/GO, 74.605-010, Brazil*

[*] *University of Brasília, Brasília/DF, 72.444-240, Brazil*

Abstract: *Cardiovascular diseases lead the world ranking of causes of death. The ubiquitous health monitoring is essential because it allows for an early diagnosis and prevents fatalities. Physiological variables that provide information about the cardiovascular system can be estimated by the photoplethysmographic signal (PPG), which can be recovered without contact with the camera. This work presents software capable of estimating physiological variables from the PPG signal obtained by a camera. They are also features implemented to improve the usability of the software.*

Keywords: *Pulse Transit Time, Pulse Wave Speed, Oxygen Saturation, Blood Pressure, Camera, Non-Contact*

I. INTRODUCTION

Cardiovascular diseases between 1990 and 2017 led the world ranking of causes of death [1]. Early diagnosis allows risk prediction and can prevent fatalities. To achieve this goal, daily monitoring of cardiovascular health is necessary. Information on Pulse Transit Time (PTT), Pulse Wave Speed (PWV), Blood Pressure (BP), and Oxygen Saturation (SpO_2) are essential for monitoring cardiovascular health. BP and SpO_2 are two of the five vital signs considered vital for monitoring hospitalized patients [2], while PWV, estimated from PTT, is one of the markers of arterial stiffness. Arterial stiffness can cause cardiovascular diseases, such as hypertension and vascular embolism [3]. Monitoring these variables allows assessing cardiovascular health and providing a prognosis for the user.

PTT is defined as the time required for a pressure wave to propagate between two arterial sites [4]. It can be used to monitor PWV, as both have an inversely proportional relationship. PWV is the speed that the pressure wave propagates along the arterial branch, being considered the gold standard for measuring arterial stiffness [5]. According to the arterial branch, where the pressure wave was measured, the estimation of PWV can be performed in two different ways.

PWV measured in two different arteries, as in the carotid and femoral arteries, are called regional PWV. It provides the mean PWV, obtained in different arteries with other mechanical characteristics [5]. The regional PWV and PTT have some limitations, as their measurements vary due to the pre-ejection period. In this case, the measurement of these variables disregards the effects caused by the reflection of the wave in the arteries, and their estimates are subject to errors in the calculation of the distance between the measurement sites [6]. These problems generate constant calibration in the devices used for measurement, limiting their use [7].

When the measurement is performed on a small arterial segment, the PWV is called Local PWV (LPWV) [8]. Some studies have reported that LPWV presents the actual speed of propagating the pulse wave in the arteries. Therefore, a more reliable estimate of the pulse wave rate [6] [5]. Besides, local measurement avoids calculation errors in the distance between the two measurement sites and allows a regional analysis of arterial stiffness.

BP is the pressure generated by the blood flow in the arterial walls. It is measured through systolic blood pressure (SBP) and diastolic blood pressure (DBP), that is, by the ratio of SBP/DBP [9]. A process commonly performed in offices is the screening for hypertension, which consists of performing at least two BP measurements and calculating the mean BP [10]. If the mean SBP exceeds 140 mmHg and/or the mean DBP exceeds 90 mmHg, the patient can be considered hypertensive [4]. It is reported in several studies that BP is directly related to PWV [5] [8] and PTT [4] [11] and can be measured using these variables, thus allowing ubiquitous BP monitoring.

SpO_2 measures the relative concentration of oxygenated hemoglobin in the blood concerning the total hemoglobin amount [12]. It is commonly used to monitor a patient's health because it provides continuous oxygen concentration measurements in the blood. Usually, a healthy person has a saturation in the range of 95% to 100%. SpO_2 levels continuously below 90% may indicate problems with oxygen distribution [13].

The physiological variables LPWV and SpO_2 can be estimated using photoplethysmographic signals (PPG) [6] [12] [13] [14]. LPWV is evaluated using two separate PPG sensors at a known distance [14]. LPWV is calculated using the ratio between the length and the PTT of the pressure wave between the PPG sensors [6] [14]. SpO_2 is computed using the pulse oximetry technique, which considers the difference in light absorption by oxygenated hemoglobin in the wavelengths of red and infrared light [13].

However, the devices commonly used to monitor these variables are only available in hospital settings. Besides, this equipment's operation requires sensors in contact with the skin, which can cause discomfort and limit the patient's movement. However, it is possible to replace PPG sensors with contact with a video camera and ambient light and recover the PPG signal using a non-contact technique [15].

In the literature, some studies acquire the SpO_2 and PWV/PTT variables from the PPG signal. Some of them are discussed in the following paragraphs.

Sugita et al. [11] obtained PTT from video images and then correlated it with BP. In this work, the researchers found a positive correlation rate of approximately 0.6 between the time difference measured on the face and palm with the BP obtained by a pressure sensor placed on the individual's left middle finger. Similarly, Khong, Rao, and Mariappan [10] used the estimated PWV through chest and forehead video to measure BP. They obtained an absolute mean error between the method evaluated at work and the oscillometric device used to compare 4.22 ± 3.15 mmHg for SBP and 3.24 ± 2.21 mmHg for DBP. Both studies obtained the PPG signal in a non-contact environment using a camera, but neither performed the LPWV evaluation.

However, Nabeel et al. [8] and P. et al. [14] performed the LPWV assessment in a small arterial segment. P. et al. [14] obtained the LPWV in the range of 2.13 to 3.23 m/s for participants aged 22 to 26 years, while Nabeel et al. [8] received the LPWV of 2.63 ± 0.42 m/s in a population aged 24.5 ± 4 years. Both were able to acquire PPG signals in the same arterial segment, calculate the pulse wave transit time, and finally estimate the LPWV. However, in both studies, PPG sensors with contact were used.

Kong et al. [16] and Shao et al. [13] measured oxygen saturation without contact from a camera. Kong et al. [16] found an error between the evaluated method and the comparison device in just three heartbeats. Shao et al. [13] found a correlation coefficient of 0.936 between the evaluated and the comparison instruments. However, in both studies, the camera was synchronized with an array of LEDs with two different wavelengths. The use of dedicated lighting made the system dependent on external hardware. In a study using only one camera, Guazzi et al. [12] found a correlation coefficient of 0.85 between the proposed method and the comparison instrument. However, the technique was limited to detecting changes in oxygen saturation and did not measure oxygen saturation.

Therefore, the present work aims to explore the estimation of the physiological variables PWV, PTT, SpO_2, and BP through a camera. Besides, it improves and adds new features to the HRVCam (Heart Rate Variability by Camera) software, now called CCM (Contactless Cardio Monitor). HRVCam was initially developed by Souza [17] and validated by Martins [18]. In the beginning, HRVCam estimated and presented heart rate (HR) and heart rate variability (HRV). Currently, CCM is also able to assess LPWV, SpO_2, and BP. In addition to evaluating the acquired signal and generating reports on the physiological variable and the BP calibration process. It also allows the measurement of the distance between regions of interest, ROIs, without contact, and enables them to carry out the LPWV/PTT calibration process for BP.

II. MATERIALS AND METHODS

A. Software Description and Signal Acquisition

The software functionalities and the acquisition of new variables were raised and evaluated in meetings held by the research group BESt (Biomedical Engineering and Embedded Systems) Group, from Pontifical Catholic University of Goias (PUC Goiás), and with future users. The software was developed in MATLAB (The Mathworks, Inc.) for being an easy-to-use programming language, in addition to having many toolboxes and packages that facilitate data acquisition and analysis.

In the tests carried out to verify the functionalities developed, a Camera (HD Pro C9200 Logitech Inc.) was used with a sampling frequency of 30 Hz (30 frames per second, fps). In all tests, the videos were recorded with a duration of 1 minute, with 800x448 pixels of resolution. The software was run on a Lenovo IdeaPad 330-15IKB laptop, equipped with Intel® Core™ i5-8250U 1.60 GHz, 8 GB of RAM, and NVIDIA GeForce® MX150 2 GB video card, with Windows 10 operating system version 20H2.

Before starting to acquire data from the user, the software's initial screen is presented to the user, as shown in Figure 1. The software works online, receiving and processing the video simultaneously, or offline, allowing the user to enter a saved video on your computer's hard disk drive. Initially, the physiological variable presented is LPWV, but the user can configure the software to show the other variables Heart Rate and its variability, BP, and SpO_2. Besides, the user can enter his anthropometric data (Figure 2) or configure the system (camera, video, and signal processing parameters) and select the variable to be estimated (Figure 3). After configuring the software, the user chooses the ROI(s) and starts acquiring the video to assess the previously selected variable. Figure 1 shows the configured software and ROIs for LPWV estimation. The following sections show the acquisition of the variables and the other functionalities of the software.

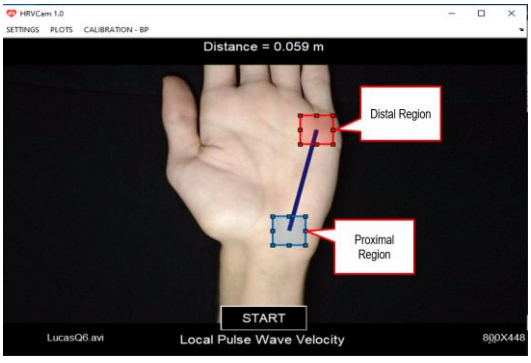

Fig 1: Initial software interface and example of ROIs for LPWV estimation

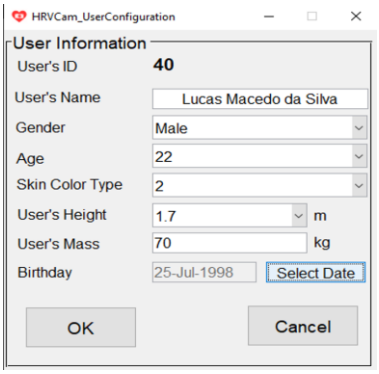

Fig 2: User data input interface

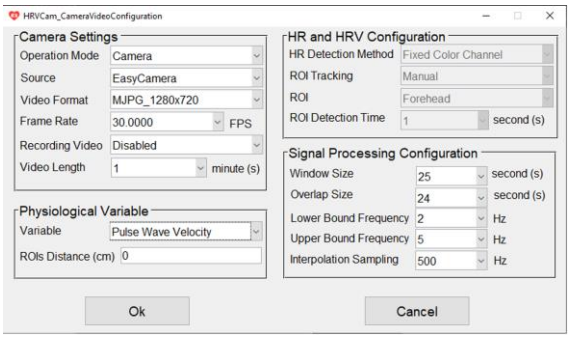

Fig 3: Camera, video, and physiological variable configuration interface

B. Local Pulse Wave Velocity

For LPWV estimation, only the frames referring to the green color channel of the video were used. Figure 4 illustrates the video processing for LPWV acquisition. In each frame, the average of the pixels in the ROI is used to compose the raw signal x [n] (Figure 4b). A high-pass filter with a cut-off frequency of 0.3 Hz is then applied at x [n] based on the previous smoothness approach [19] to remove noise caused by the user's movement. The signal is then normalized, subtracting its mean (xm) and dividing by its standard deviation (∂), as shown in equation 1, generating the signal z [n].

$$z[n] = (x[n] - xm) / \partial \quad (1)$$

A Chebyshev type II low-pass filter with a cut-off frequency of 5 Hz was applied to the z [n] signal. Finally, the signal sampled at 30 Hz is interpolated to 500 Hz to simulate a high sampling rate. The resulting signal, y [n], is like the signal obtained from sensors with contact, as shown in the work of [14].

In this way, the pre-processing output, y [n], contains the two PPG signals used to calculate the LPWV. The calculation is performed by calculating the distance between the two ROIs (Δd) and the average time difference between two peaks of the PPG signal obtained in the two ROIs (Δt). Equation 2 shows the LPWV calculation,

$$LPWV = \Delta d / \Delta t \quad (2)$$

the value of Δt is calculated as described by equation 3, where Ti indicates the time difference between the peaks of the two signals obtained in the two ROIs and n is the number of peaks found. The value obtained is used as an index equivalent to the PTT.

$$\Delta t = (|T_1| + |T_2| + ...+ |T_n|)/n \quad (3)$$

An intelligent peak combination algorithm is applied to avoid a peak from occurring in just one of the signals or the occurrence of two peaks with a large difference in time (as highlighted in Figure 4c). The algorithm combines the peaks of two signals with a time difference less than or equal to 0.1 second [20]. Figure 4d shows an example of disregarded peaks, as the time difference between them was large, which would be impossible to occur at a distance Δd.

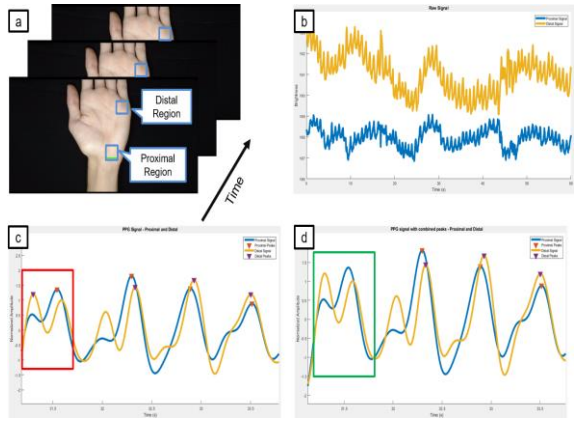

Fig 4: (a) Acquisition of the online signal. (b) The raw signal was obtained in the two regions of interest (proximal in blue and distal in yellow). (c) Signal received after processing. (d) Peaks after going through the peak combination algorithm

C. Calculation of the Distance Between the Regions of Interest

The software has a feature that calibrates the distance (in pixels) between the two ROIs for the length (cm) between them. Figure 5 shows the algorithm for the calibration. The user informs the physical distance between the two ROIs (physDist) at the measurement site. The software then calculates the distance in pixels between the ROIs (pixelDist) and a calibration factor that relates the two lengths (calibration factor). The factor is the ratio of the reported distance to the calculated distance. This factor is saved in case the user moves one of the ROIs, updating the distance value.

```
physDist ← distance entered by the user (in cm)
pixelDist ← distance between the center of the two ROIs (in pixels)
calibration factor ← pixelDist / physDist
Save calibration factor
```

Fig 5: Algorithm for distance calibration

Whenever the user moves one of the two ROIs, the stored factor variable is recovered. The relationship between the distance from the center of the two ROIs (roisDist) and the factor variable is the physical distance between them in centimeters. Figure 6 shows the algorithm to perform this process. The resulting value is multiplied by 0.01 to convert from centimeter to meter.

```
factor ← load calibration factor
roisDist ← distance between the center of the two ROIs (in pixels)
distance ← (pixelDist / factor) * 0.01
```

Fig 6: Algorithm for calculating the new distance

D. Oxygen Saturation

Oxygen saturation is estimated by the PPG signal obtained in the palm. In each frame of the video, the average ROI pixels make up the signal, like the x [n] signal shown in section 2.2. The red and green color channels are used as the red and infrared wavelengths, respectively.

The recovered PPG signal consists of two components. A pulsatile component, AC (Alternating Current), which is attributed to synchronous blood variation, and a DC (Direct Current) feature, which is related to low-frequency components in blood flow [21]. The ratio between the AC and DC components of the two wavelengths is defined as the ratio of the ratios (RR) (equation 4). The RR value is proportional to the oxygen saturation (SpO_2) value (equation 5) [13],

$$RR = (AC_{red} / DC_{red}) / (AC_{green} / DC_{green}) \quad (4)$$

$$SpO_2 = A * RR + B \quad (5)$$

where A and B are constants calibrated with a comparison instrument. In the present work, the Mediclini AS-302-L pulse oximeter was used for the calibration process described in section 3.2.

The DC component is recovered by a Butterworth low-pass filter of order two and a cut-off frequency of 0.7 Hz. The AC component is retrieved by a Butterworth band-pass filter of order one and cut-off frequency from 0.7 to 3 Hz. Right after separation of the elements, in time windows of 4 seconds and without overlap, the peak-to-peak value is calculated in the AC component. The average of the signal is calculated in the DC component. Then the RR value is calculated, according to equation 4. Finally, a moving average of 10 seconds is applied to the RR value, thus obtaining the RR value estimated by the software in time windows of 4 seconds each.

E. Blood Pressure

The software has a feature to facilitate the calibration of LPWV or PTT for BP estimation. The interface that implements the functionality was developed with the MATLAB interface design toolbox. It features buttons, lists, and graphs that allow interaction with the user. Figure 7 presents the graphical interface with blood pressure data loaded by the user. Besides, at the end of the calibration process, a report is generated containing all the data and parameters used.

For the calibration process, there are two modes of operation. In manual mode, the user selects the curve and its degree and then generates the calibration curve. The available curves are polynomials, a/x + b type curves, logarithmic curve, and exponential curve. All coefficients of the curve are found with the MATLAB adjustment function. The second mode of operation is the automatic mode, in which the user informs the type of error between the measured and estimated values to select the best curve. The types of error can be the mean square error (MSE), the square root of the mean square error (RMSE), or the mean absolute error (MAE).

In automatic mode and possession of the input data, the software generates several curves, calculates the chosen error value, and selects the curve with the smallest error. Regardless of the mode of operation, the software enables the dispersion graphs editions after plotting the curves, which can be the graph of the curve and correlation coefficients (Figure 13a), the absolute error graph (Figure 13b), or the Bland Altman graph [22].

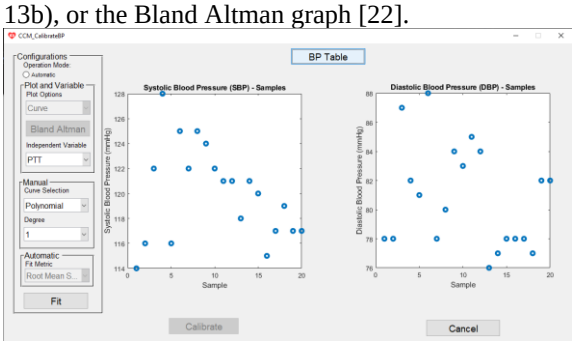

Fig. 7: Initial interface for BP calibration

F. Signal Evaluation and Report Generation

During data acquisition, the quality of the PPG signal is displayed. The raw signal is evaluated using the signal-to-noise ratio (SNR) every 10 seconds of acquisition. Quality is defined as Bad if the SNR is less than -2 dB; Good if the SNR is more significant than -2 dB; and less than 0 dB or Excellent, otherwise.

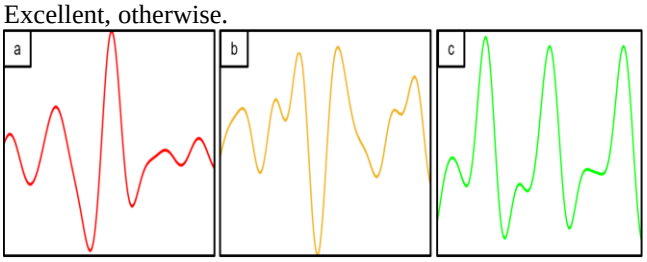

Fig. 8: (a) Example of Bad quality signal. (b) Example of Good quality signal. (c) example of Excellent quality signal

If the signal is rated as Bad, it indicates that it has a lot of noise. This fact is related to the user's movements. Thus, the use of this sign to estimate variables is not recommended for estimating variables. When evaluated as Good, the noise signal has, but can still be used to estimate the variables. In this case, the noise influences only a part of the signal. Finally, if the signal is rated as Excellent, it has sufficient quality to calculate variables and has little effect by the noise. This functionality allows the user to have feedback on the acquired signal's quality, allowing him to start the acquisition if he wants to obtain the signals with more quality. Figure 8 shows sections of the signal classified as Bad (Figure 8a), Good (Figure 8b), and Excellent (Figure 8c).

The software also generates reports containing information on the estimation of variables and the BP calibration process. The data used for the reports are those

informed in the user configuration (Figure 2) and camera/video configuration (Figure 3) interfaces or the data related to the calibration process. The report is generated from the MATLAB *mlreportgen* package. The base document for the report was created with Microsoft Word. The software fills the document fields with the input data and the input variable, generates the information in PDF format, and makes it available to the user. Figure 9 shows an example of the LPWV estimate report generated by the software.

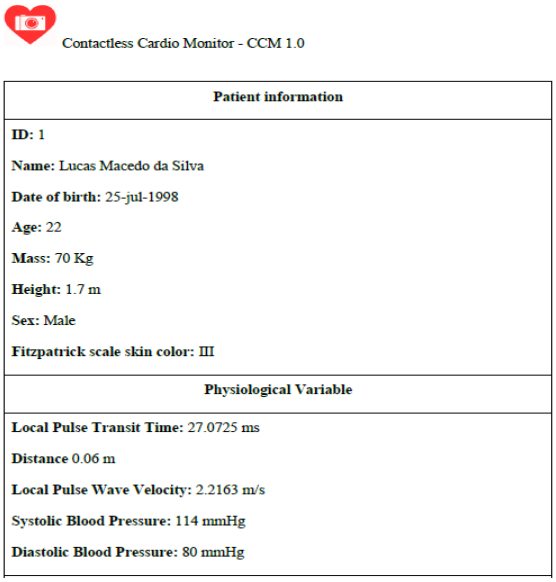

Contactless Cardio Monitor - CCM 1.0

Patient information
ID: 1
Name: Lucas Macedo da Silva
Date of birth: 25-jul-1998
Age: 22
Mass: 70 Kg
Height: 1.7 m
Sex: Male
Fitzpatrick scale skin color: III
Physiological Variable
Local Pulse Transit Time: 27.0725 ms
Distance 0.06 m
Local Pulse Wave Velocity: 2.2163 m/s
Systolic Blood Pressure: 114 mmHg
Diastolic Blood Pressure: 80 mmHg

Fig. 9: Example of a report generated by the software

III. RESULTS AND DISCUSSIONS

A. *Estimated Local PWV*

A test was carried out with three participants with different skin color levels on the Fitzpatrick scale to verify PPGs signals' acquisition to calculate LPWV, [23]. The objective was to confirm that the recovered signals had all the characteristic points of a PPG signal and that the signal peaks were visible.

The characteristic points considered are the beginning/end of the pulse wave, the systolic peak, and the diastolic peak. Thus, the beginning/end of the pulse wave represents the moment when the pressure wave begins or ends, the systolic peak marks the moment when blood is ejected into the arteries. The diastolic peak marks the instant when the heart fills up with blood from the veins [15]. These points show events in the cardiac cycle and are an essential part of the PPG signal waveform. They were used to check if the recovered signal had a waveform like the PPG signal obtained by sensors with contact.

The individuals were separated into two groups, according to age. Group 1 consisted of individual 1 at 22 years of age, while group 2 consisted of individuals 2 and 3 at 55 years. The distance between the center of the two ROIs was calculated using the non-contact method presented in Section 2 to estimate the LPWV. The values were validated with a tape measure, and the absolute error between the two instruments was only in the 4th decimal place. The distance used was 0.06 m for individuals 1 and 3 and 0.07 m for individual 2.

a) Group 1 - Individual 1: Individual 1 was 22 years old, male, had no history of cardiovascular disease, and had level III on the Fitzpatrick scale. Figure 10 shows a section of the acquired signal. As highlighted, the signal reflected all the PPG signal's characteristic points, and the peaks (red circles) are easily identifiable. For this individual, the Δt value was 0.0268 s, and the LPWV was 2.23 m/s. The result is in line with those obtained by Nabeel et al. [8] and P. et al. [14] for a population aged 21 to 28, which corresponds to the individual's age group (22 years).

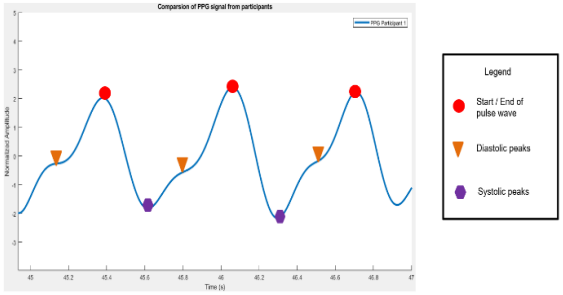

Fig. 10: PPG signal acquired in the individual 1

***b) Group 2 - Individuals 2 and 3*:** Individuals 2 and 3 were 55 years old, a man and a woman, with no history of cardiovascular disease, level V (male) and level II (female) on the Fitzpatrick scale. Figure 11 shows a section of the two individuals' signals, with the man in Figure 11a and the woman in Figure 11b. In this group, the peaks were also visible, as well as the other characteristic points. Besides, the dicrotic notch (slight depression between the systolic and diastolic peaks) became smaller. This characteristic was expected, as increasing age causes the distance between the peaks to decrease, and the dicrotic notch becomes less visible [15].

For women, the Δt value was 0.0281 s, and the LPWV was 2.13 m/s, while for men, the Δt value was 0.0260 s and the LPWV was 2.69 m/s.

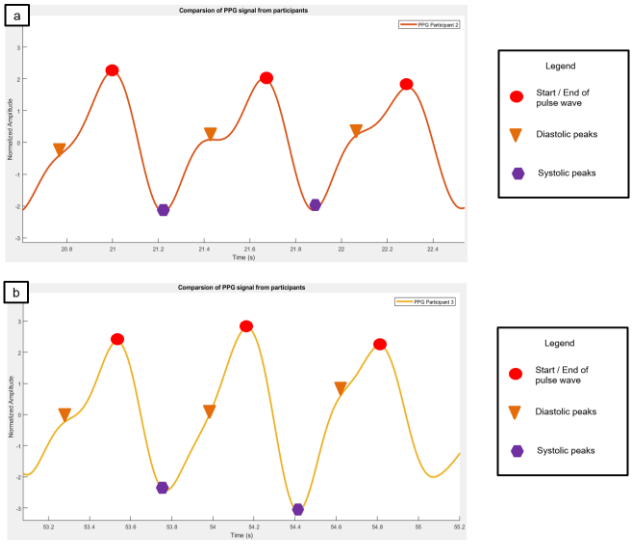

Fig. 11: (a) PPG signal acquired for individual 2. (b) PPG signal acquired for individual 3

c) Comparison of Group 1 and Group 2: For the three individuals, the recovered signals had the PPG signal waveform characteristics and, the peaks (red circles) were easily identifiable. Besides, the signal recovered in an individual with scale V presented a waveform similar to an individual with scale II and III. This fact corroborates the palm as ROI, as it allows the acquisition of signals in people with a higher melanin concentration. Therefore, the distal region is just below the little finger, and the proximal region is located above the wrist 6 ~ 7 cm away from the distal region.

The main limitation of this test was a small population, n = 3. The population has different characteristics, which allows an evaluation of the software in different scenarios. In the future, it is expected to conduct tests on a more extensive and more diverse population to validate the acquisition of LPWV without contact.

B. SpO_2 Calibration

For the calibration process of RR values with SpO_2 values, videos of a single 22-year-old individual with no history of cardiovascular diseases were captured. During acquisition, SpO_2 values were obtained by the Mediclini AS-302-L pulse oximeter. The values obtained by the software and by the oximeter were noted, and Pearson's correlation coefficient was calculated between them. The coefficient found was r = -0.75. The values of constants A and B in Equation 5 were calculated using the Matlab polyfit function. Equation 6 shows the regression obtained.

$$SpO_2 = -22.93*RR + 106.611 \quad (6)$$

After calibration, a test was performed with the software. Figure 12 shows the SpO_2 graph obtained with the two instruments. The values of the comparison instrument, in blue, and the SpO_2 value calculated by the software, in red. As can be seen, the values were very close. The average absolute error was 0.21667%. The software took longer than the reference oximeter to capture the change in saturation. This may be related to the position of the hand. As it was lifted, the pressure wave took longer to reach the region of interest. Besides, the values estimated by the software have been rounded, as the reference oximeter does not have decimal values.

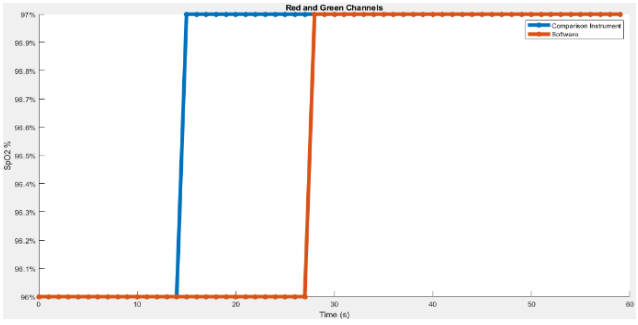

Fig. 12: Estimation of SpO_2 with both instruments, in red the value estimated by the software and in blue by the oximeter

However, the absolute error between the two instruments' samples did not exceed 1%, which is within the limits of clinically acceptable precision, i. e., accuracy less than 4% in the measurement range of 70 -100% SpO_2 [24].

The major limitation of the SpO_2 estimate in the present study was the acquisition of data for system calibration. Therefore, in the future, it is intended to improve accuracy by acquiring more data to calibrate the software, in addition to developing an interface for the calibration of RR and SpO_2 values, similar to the BP calibration interface. Another limitation, which also extends to LPWV estimation, was using a 30 Hz (30 fps) sampling camera for signal acquisition. The acquisition rate can influence the detection of changes in the signal on the skin. Thus, in future research, it is intended to employ a camera with a higher sampling frequency.

C. Interface Test for BP Calibration

For testing the functioning of the BP calibration interface, 15 videos were collected from a single 22-year-old individual with no history of cardiovascular disease. The PWV and PTT values were estimated by the software and saved automatically in a table. The SBP and DBP values were calculated by the Omron HEM-7122 BP Monitor and recorded manually in a second table. Both instruments were started at the same time.

After acquiring the data, they were loaded into the calibration interface (Figure 7a). After this step, it was verified that all components of the code were operating as expected. Also, it was demonstrated that the report with the input data was generated and that the software was calibrated correctly. Figure 13 shows the interface after the data has been loaded, and the calibration curve has been developed in automatic mode. Figure 13a shows the calibration curve, the Pearson (r) and Spearman (p) coefficients. Figure 13b shows the absolute error graph between the instrument and the software.

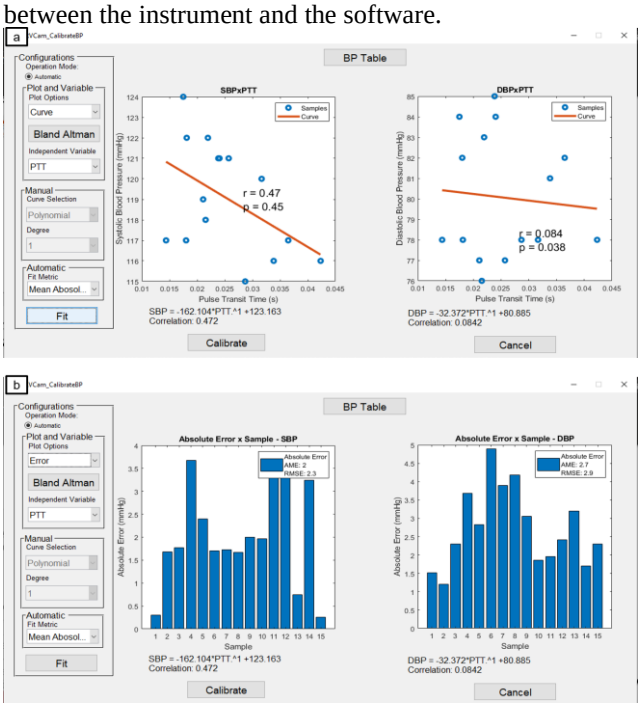

Fig. 13: (a) Graphical interface with the generated curve. (b) Graphical interface with the absolute error graph

The interface development's main objective was to simplify the software calibration process, bringing the parameters from the interface elements closer to the user. It makes it possible to improve the measurement accuracy and allows the user to add new data whenever necessary. Besides, the interface presents useful information that can be used in future validation studies of this software.

In the test performed with the automatic operation mode, a polynomial of the first degree was found to calibrate the PTT for BP. Calculation using polynomials costs less computationally compared to other curves. For the data set, the mean absolute error between the instrument and the software for SBP was 2 mmHg, while for DBP it was 2.7 mmHg. The mean absolute error was relatively low, which corroborates the use of calibration that allows estimating BP from PTT/LPWV.

It is intended to acquire more data in a larger population and with different characteristics and use the interface to calibrate the curve in future work. Besides, validation studies and analysis of the relationship between LPWV/PTT and BP.

IV. CONCLUSION

The present work presented the development of software for estimating and calibrating non-contact physiological variables. The resources developed will allow the user to interact with the software and obtain more information about their cardiovascular health and improve BP estimation accuracy with new data. The possibility of calibrating the distance allows the distance between the ROIs without contact with the user's skin. The software could acquire two PPG signals without contact in a small arterial segment and then estimate the LPWV. It was also calibrated to estimate SpO_2, with a correlation coefficient of $r = 0.75$. In all cases, the palm region was used to acquire the signals. The palm allows the acquisition of the PPG signal in people with a higher melanin concentration. Future work will focus on: i) testing a larger population with normotensive and hypertensive individuals with comparison instruments; ii) improve the calculation of the contactless distance to eliminate the need for the calibration step; iii) in the acquisition of new BP and SpO_2 data to improve the software's accuracy in estimating these variables.

ACKNOWLEDGMENTS

The authors would like to thank the members of BESt Group and external collaborators, especially Arthur Galdino, Higor Alves, and Vitor de Almeida, Edna Lúcia Macedo, and Francisco Moreira.

REFERENCES

[1] Share of deaths by cause. (n.d.). Our World in Data. Retrieved December 1, 2020, from https://ourworldindata.org/grapher/share-of-deaths-by-cause

[2] Araujo, L. C. de, & Romero, B. (2015). Pain: evaluation of the fifth vital sign. A theoretical reflection. Revista Dor, 16(4). https://doi.org/10.5935/1806-0013.20150060

[3] Deng, L., Zhang, Y., & Mo, H. (2018). Evaluation of TT-Based Local PWV Estimation for Different Propagation Velocities. Proceedings of the 2018 5th International Conference on Biomedical and Bioinformatics Engineering - ICBBE '18. https://doi.org/10.1145/3301879.3301894

[4] Mukkamala, R., & Hahn, J.-O. Toward Ubiquitous Blood Pressure Monitoring via Pulse Transit Time: Predictions on Maximum Calibration Period and Acceptable Error Limits. IEEE Transactions on Biomedical Engineering, 65(6), (2018) 1410–1420. https://doi.org/10.1109/tbme.2017.2756018

[5] Pereira, T., Correia, C., & Cardoso, J. Novel Methods for Pulse Wave Velocity Measurement. Journal of Medical and Biological Engineering, 35(5), (2015) 555–565. https://doi.org/10.1007/s40846-015-0086-8

[6] Nabeel, P. M., Jayaraj, J., & Mohanasankar, S. Single-source PPG-based local pulse wave velocity measurement: a potential cuffless blood pressure estimation technique. Physiological Measurement, 38(12), (2017) 2122–2140. https://doi.org/10.1088/1361-6579/aa9550

[7] Kiran V., R., P.M., N., Joseph, J., Shah, M. I., & Sivaprakasam, M. Evaluation of Local Pulse Wave Velocity using an Image Free Ultrasound Technique. 2018 IEEE International Symposium on Medical Measurements and Applications (MeMeA). https://doi.org/10.1109/memea.2018.8438649

[8] P M, N., Karthik, S., Joseph, J., & Sivaprakasam, M. Arterial Blood Pressure Estimation From Local Pulse Wave Velocity Using Dual-Element Photoplethysmograph Probe. IEEE Transactions on Instrumentation and Measurement, 67(6), (2018) 1399–1408. https://doi.org/10.1109/tim.2018.2800539

[9] Myint, C., Lim, K. H., Wong, K. I., Gopalai, A. A., & Oo, M. Z. (2014). Blood Pressure measurement from Photo-Plethysmography to Pulse Transit Time. 2014 IEEE Conference on Biomedical Engineering and Sciences (IECBES). https://doi.org/10.1109/iecbes.2014.7047550

[10] Khong, W. L., Rao, N. S. V. K., & Mariappan, M. (2017). Blood pressure measurements using non-contact video imaging techniques. 2017 IEEE 2nd International Conference on Automatic Control and Intelligent Systems (I2CACIS). https://doi.org/10.1109/i2cacis.2017.8239029

[11] Sugita, N., Obara, K., Yoshizawa, M., Abe, M., Tanaka, A., & Homma, N. (2015). Techniques for estimating blood pressure variation using video images. 2015 37th Annual International Conference of the IEEE Engineering in Medicine and Biology Society (EMBC). https://doi.org/10.1109/embc.2015.7319325

[12] Guazzi, A. R., Villarroel, M., Jorge, J., Daly, J., Frise, M. C., Robbins, P. A., & Tarassenko, L. (2015). Non-contact measurement of oxygen saturation with an RGB camera. Biomedical Optics Express, 6(9), 3320. https://doi.org/10.1364/boe.6.003320

[13] Shao, D., Liu, C., Tsow, F., Yang, Y., Du, Z., Iriya, R., Yu, H., & Tao, N. (2016). Noncontact Monitoring of Blood Oxygen Saturation Using Camera and Dual-Wavelength Imaging System. IEEE Transactions on Biomedical Engineering, 63(6), 1091–1098. https://doi.org/10.1109/TBME.2015.2481896

[14] P., M., W., A., H., P., & M., T. (2020). A Photoplethysmographic Monitor for Local Pulse Wave Velocity Measurement. International Journal of Computer Applications, 177(31), 62–67. https://doi.org/10.5120/ijca2020919811

[15] McDuff, D., Gontarek, S., & Picard, R. W. Remote Detection of Photoplethysmographic Systolic and Diastolic Peaks Using a Digital Camera. IEEE Transactions on Biomedical Engineering, 61(12), (2014) 2948–2954. https://doi.org/10.1109/tbme.2014.2340991

[16] Kong, L., Zhao, Y., Dong, L., Jian, Y., Jin, X., Li, B., Feng, Y., Liu, M., Liu, X., & Wu, H.. Non-contact detection of oxygen saturation based on visible light imaging device using ambient light. Optics Express, 21(15), (2013) 17464. https://doi.org/10.1364/oe.21.017464

[17] SOUZA, P. H. B. (2019). Método para estimação da frequência cardíaca e variabilidade cardíaca com base em fotopletismografia por vídeo. Dissertação de Mestrado em Engenharia Biomédica, Publicação 109A/2019, Programa de Pós-Graduação em Engenharia Biomédica, Faculdade Gama, Universidade de Brasília, Brasília, DF, 154p.

[18] MARTINS, P. C. M. L. Validação do software HRVCam para avaliação da frequência cardíaca e da variabilidade da frequência cardíaca. 2019. Dissertação de Mestrado (Mestrado em Atenção à Saúde), Pontifícia Universidade Católica de Goiás, Goiânia.

[19] Tarvainen, M. P., Ranta-aho, P. O., & Karjalainen, P. A. An advanced detrending method with application to HRV analysis. IEEE Transactions on Biomedical Engineering, 49(2), (2002) 172–175. https://doi.org/10.1109/10.979357

[20] SOUZA, Pedro H. B., SOUZA, Israel. M. B., ALCALÁ, Symone G. S., VITORINO, Priscila V. de O., BARBOSA, Talles M. G. de A., ROCHA, Adson F. da. (2020). Video-based Photoplethysmography and Machine Learning Algorithms to Achieve Pulse Wave Velocity [Unpublished manuscript]. School of Exact and Computer Sciences, Pontifical Catholic University of Goiás.

[21] Naeini, E. K., Azimi, I., Rahmani, A. M., Liljeberg, P., & Dutt, N. A Real-time PPG Quality Assessment Approach for Healthcare Internet-of-Things. Procedia Computer Science, 151, (2019) 551–558. https://doi.org/10.1016/j.procs.2019.04.074

[22] Giavarina, D.. Understanding Bland Altman analysis. Biochemia Medica, 25(2), (2015) 141–151. https://doi.org/10.11613/bm.2015.015

[23] Fitzpatrick, T. B. The validity and practicality of sun-reactive skin types I through VI. Archives of Dermatology, 124(6), (1988) 869–871. https://doi.org/10.1001/archderm.124.6.869

[24] van Gastel, M., Stuijk, S., & de Haan, G. A new principle for measuring arterial blood oxygenation, enabling motion-robust remote monitoring. Scientific Reports, 6(1) (2016). https://doi.org/10.1038/srep38609